Pressure-flow curve derived from coronary CT angiography for detection of significant hemodynamic stenosis

Xie, X.Z.; Wen, D.D.; Zhang, R.C.; Tao, Q.; Wang, C.; Xie, S.Y.; ... ; Zheng, M.W.

European Radiology (2020) 30:4347–4355
https://doi.org/10.1007/s00330-020-06821-w

CARDIAC

Pressure-flow curve derived from coronary CT angiography for detection of significant hemodynamic stenosis

Xinzhou Xie[1] · Didi Wen[2] · Ruichen Zhang[1] · Qian Tao[3] · Ce Wang[4] · Songyun Xie[1] · Hui Liu[4] · Minwen Zheng[2]

Received: 9 December 2019 / Revised: 2 March 2020 / Accepted: 18 March 2020 / Published online: 2 April 2020

Abstract

Objectives Coronary CT angiography (cCTA) has been used to non-invasively assess both the anatomical and hemodynamic significance of coronary stenosis. The current study investigated a new CFD-based method of evaluating pressure-flow curves across a stenosis to further enhance the diagnostic value of cCTA imaging.

Methods Fifty-eight patients who underwent both cCTA imaging and invasive coronary angiography (ICA) with fractional flow reserve (FFR) within 2 weeks were enrolled. The pressure-flow curve–derived parameters, viscous friction (VF) and expansion loss (EL), were compared with conventional cCTA parameters including percent area stenosis (AS) and minimum lumen area (MLA) by receiver operating characteristic (ROC) curve analysis. FFR ≤ 0.80 was used to indicate ischemia-causing stenosis. Correlations between FFR and other measurements were calculated by Spearman's rank correlation coefficient (rho).

Results Sixty-eight stenoses from 58 patients were analyzed. VF, EL, and AS were significantly larger in the group of FFR ≤ 0.8 while smaller MLA values were observed. The ROC-AUC of VF (0.91, 95% CI 0.81–0.96) was better than that of AS (change in AUC (ΔAUC) 0.27, $p < 0.05$) and MLA (ΔAUC 0.17, $p < 0.05$), and ROC-AUC of EL (0.90, 95%CI 0.80–0.96) was also better than that of AS (ΔAUC 0.26, $p < 0.05$) and MLA (ΔAUC 0.16, $p < 0.05$). FFR values correlated well with VF (rho = − 0.74 (95% CI − 0.83 to − 0.61, $p < 0.0001$) and EL (rho = − 0.74 (95% CI − 0.83 to − 0.61, $p < 0.0001$).

Conclusion Pressure-flow curve–derived parameters enhance the diagnostic value of cCTA examination.

Key Points

- *Pressure-flow curve derived from cCTA can assess coronary lesion severity.*
- *VF and EL are superior to cCTA alone for indicating ischemic lesions.*
- *Pressure-flow curve derived from cCTA may assist in clinical decision-making.*

Keywords Coronary artery disease · CT angiography · Hemodynamics

✉ Hui Liu
liuhuijiujiu@gmail.com

✉ Minwen Zheng
zhengmw2007@163.com

[1] Department of Information Engineering, Northwestern Polytechnical University, Xi'an, Shaanxi, People's Republic of China

[2] Department of Radiology, Xijing Hospital, The Fourth Military Medical University, Xi'an, Shaanxi, People's Republic of China

[3] Department of Radiology, Leiden University Medical Center, Leiden, The Netherlands

[4] Department of Radiology, Guangdong Provincial People's Hospital, Guangdong Academy of Medical Sciences, Guangzhou, Guangdong, People's Republic of China

Abbreviations

AS	Area stenosis
AUC	Area under the receiver operator characteristic curve
CAD	Coronary artery disease
cCTA	Coronary computed tomographic angiography
CDP	Pressure drop coefficient
CFD	Computational fluid dynamic
EL	Expansion loss
FFR	Fractional flow reserve
FFR-CT	Fractional flow reserve derived from coronary computed tomographic angiography
HU	Hounsfield units
ICA	Invasive coronary angiography
MLA	Minimum lumen area
Rho	Spearman's rank correlation coefficient

ROC	Receiver operating characteristic
ROI	Region of interest
VF	Viscous friction

Introduction

Accurate assessment of coronary physiology to guide decision-making in cardiac catheterization is a persistent challenge for interventional cardiologist [1]. Currently, fractional flow reserve (FFR) is considered as the gold standard for physiological assessment of coronary lesion severity [2–4]. However, FFR measurement is invasive and requires pharmacologic intervention, which limits its in-hospital utilization [5]. Coronary computed tomography angiography (cCTA) is a non-invasive method to visualize the coronary arteries. Numerous studies have demonstrated that a negative cCTA test can effectively rule out anatomically significant stenoses [6–8]. However, the anatomical evaluation may be not consistent due to the complex relationship between anatomic lesions and the hemodynamic severity [9]. With the emergence of computational fluid dynamic (CFD) method, the anatomical models obtained by cCTA can be further analyzed to model the coronary flow at maximal hyperemia, and FFR can be estimated non-invasively (FFR-CT) [10]. FFR-CT enables determination of hemodynamically significant stenosis from cCTA images, and the accuracy depends on the modeling of distal flow resistance at maximal hyperemia [10]. However, the distal flow resistance is derived from myocardial volume (by using several empirical equations), which undergoes a considerable dynamic changes during cardiac cycle [11]. Furthermore, individuals show a wide variation of adenosine-induced changes in microvascular resistances and mean aortic pressure during FFR measurement [12]. These uncertainties highlight the need to develop an alternative method which does not rely on those empirical equations.

Pressure losses over a stenosis can be approximately determined by a common fluid dynamic equation [13]:

$$\Delta\overline{p} = VF \cdot \overline{Q} + EL \cdot \overline{Q}^2 \quad (1)$$

where $\Delta\overline{p}$ is the mean pressure drop, VF is the viscous friction, EL is the expansion loss, and $\overline{Q}$ is the mean flow rate. Recently, our group proposed a novel non-invasive method (pressure-flow curve–based method) to assess the two parameters, VF and EL [14]. Since stenosis will increase VF and EL of the stenosis section, leading to an increase in pressure drop, we hypothesize these two parameters can be used to assess hemodynamic severity of coronary stenosis (EL (or pressure drop coefficient) was already used as an invasive diagnostic parameter for determining the functional significance of a coronary stenosis [14]). Unlike FFR-CT, the pressure-flow curve–based method does not need to accurately estimate the distal flow resistance at maximal hyperemia and is a purely anatomy-derived method (does not rely on those empirical equations employed in FFR-CT) [14]. However, FFR values cannot be obtained and only the flow resistance parameters (VF and EL) can be used as an alternative. Hence, by comparing to conventional cCTA parameters including area stenosis (AS) and minimum lumen area (MLA) in patients with suspected CAD (with the invasive FFR as the gold standard), this study investigated whether this new method could enhance the diagnostic value of cCTA examination.

Materials and methods

Study population

Between January 2013 and July 2016, 64 consecutive patients with suspected coronary artery disease from 2 centers who underwent cCTA before invasive coronary angiography (ICA) with intended FFR within 2 weeks were enrolled in this retrospective study. Patients with low image quality that making it impossible to accurately reconstruct the anatomic model were excluded (significant motion in cCTA ($n = 1$); severely calcified plaque obscuring cCTA lumen ($n = 3$); excessive image noise ($n = 1$); and insufficient contrast filling ($n = 1$)).

FFR measurement

FFR is defined as the ratio between mean distal coronary pressure and mean aortic pressure; both were measured simultaneously at maximal hyperemia. Distal coronary pressure was measured with a coronary pressure guidewire (Certus Pressure Wire, St. Jude Medical). Maximal hyperemia was induced by intravenous administration of adenosine/ATP at a rate of 140 μg/kg/min [15]. Hyperemic pressure pullback tracing was performed in all diseased arteries to discriminate focal from diffuse disease. A lesion with an FFR ≤ 0.80 was considered to be functionally significant [3].

Coronary CT angiography

All cCTA scans were retrospectively performed with a second-generation 128-slice dual-source CT (Somatom Definition Flash, Siemens Healthcare). Heart rate < 90 bpm was targeted to achieve prior to scanning (by administrating oral β-blocker (50 mg, Metoprolol; Betaloc®, AstraZeneca)). Furthermore, a sublingual dose of isosorbide dinitrate 2.5 mg (Isoket; Schwarz Pharma) was also administrated 2 min before image acquisition. The scan parameters were as follows: a pitch of 0.2–0.5 adapted to the heart rate, slice collimation $2 \times 64 \times 0.6$ mm by means of z-flying focal spot, reference

tube voltage 120 kV with automatic tube voltage modulation, reference tube current 320 mAs with automatic tube current modulation, gantry rotation time 0.28 s. The image acquisition range was from 2 cm below the bifurcation of trachea to the diaphragm. With the above settings, patients were expected to expose to moderate radiation dose.

A bolus of 1 ml/kg iopromide 370 (370 mg I/ml, Ultravist 370, Bayer Schering Pharma) was injected into an antecubital vein at a flow rate of 5 ml/s, followed by 30 ml saline solution. The region of interest (ROI) was placed into the aortic root, and image acquisition started 6 s after the signal attenuation reached a threshold of 100 Hounsfield units (HU).

Images were reconstructed using a conventional FBP algorithm with a medium smooth kernel designed for cardiac imaging (B26f). All images were reconstructed with a slice thickness of 0.75 mm and increment of 0.5 mm. All data were transferred to an offline workstation (syngo MMWP VE 36A, Siemens Healthcare) for further analysis. The assessments of cCTA AS and MLA were carried out by two experienced observer (with 6 and 5 years of experience on cardiac imaging), who were blinded to the invasive FFR values. AS was calculated on the basis of proximal and distal reference segments, which were the most adjacent points to the maximal stenosis. MLA was measured from the short-axis views of double-oblique reconstructions at the maximal stenosis site. Any disagreement between the two observers was resolved by consensus. The mean values of AS and MLA measured by two observers were used for further analysis.

CFD-based pressure-flow curve and the derived parameters

Pressure-flow curve and the derived parameters were obtained with a novel method proposed by our group previously (as shown in Fig. 1) [14]. Coronary arteries were semi-automatically segmented and reconstructed in Mimics Medical (version 21.0.0.406, Materialise NV), and only the stenosis sections with nearby branches were retained for further CFD analysis. For vessels with multiple lesions, the segment was selected to match the site on which invasive FFR was measured. Steady flow simulations were performed seven times (to derive a combined pressure-flow curve for further analysis), each with a different outlet boundary condition (total distal resistance was set to be 120 mmHg s/cm^3 at first, and then reduced to 87.5, 75.0, 62.5, 50.0, 37.5, and 25.0%, respectively). The simulated pressure drops and flow rates of each steady flow simulation were combined to provide a pressure-flow curve. Finally, the VF and EL were estimated from the curve by using iterative least squares estimation for nonlinear regression [14]. In this work, ANSYS FLUENT V14 (ANSYS Inc.) was used to perform steady flow simulations.

Statistical analyses

Quantitative variables were expressed as means ± standard deviations or median with 25–75% inter-quartile range. One-sample Kolmogorov-Smirnov test was used to check the assumption of normal distribution. For normally distributed variables, the independent samples *t* test was used to compare different groups; for non-normally distributed variables, the Mann-Whitney *U* test was used to compare different groups. Receiver operating characteristic (ROC) curve analyses were performed for AS, MLA, VF, and EL. The best cutoff values for these variables were determined by Youden's index. The difference between two areas under curves (AUCs) was calculated by using the method developed by Hanley and McNeil [16]. Since data was not normally distributed, the correlations between pressure-flow curve–derived parameters (VF and EL) and invasive FFR measurements were calculated by using Spearman's rank correlation coefficient (rho). A 2-tailed p value < 0.05 was considered to be statistically significant. MedCalc statistical software (version 19.0.4; MedCalc software bvba) was used for all statistical analyses.

Results

Sixty-eight significant coronary stenotic segments in 58 patients were analyzed. Further demographics for the included 58 patients (39 male, 19 female; mean age 66.1 ± 10.4 years) were described in Table 1. The numbers of patients with single-vessel and multi-vessel disease were 48 and 10, respectively. Out of the 68 coronary arteries stenoses, 47 (67.6%) were in left anterior descending coronary artery, 11 (20.6%) in left circumflex coronary artery, and 10 (11.8%) in right coronary artery.

By using 0.8 as a cutoff value of FFR, lesions were divided into two subgroups. Compared with the group of insignificant lesions (FFR > 0.8), the VF, EL, and AS were significantly larger and MLA was significantly lower in the group of hemodynamic significant lesions (FFR ≤ 0.8) (Table 2). According to ROC curve analysis (Table 3 and Fig. 2), the ROC-AUC of VF (0.91, 95% CI 0.81–0.96) was better than that of AS (change in AUC (ΔAUC) 0.27; $p < 0.05$) and MLA (ΔAUC 0.17, $p < 0.05$), and AUC of EL (0.90, 95% CI 0.80–0.96) was also better than that of AS (ΔAUC 0.26; $p < 0.05$) and MLA (ΔAUC 0.16, $p < 0.05$). With the best cutoff values chosen for VF (0.41 mmHg s/ml) and EL (0.43 mmHg s^2/ml^2) respectively, the sensitivity, specificity, positive predictive value, and negative predictive value for hemodynamic significant lesions were presented in Table 3. The diagnosis accuracy reached 0.88 (95% CI 0.78–0.95) and 0.87 (95% CI 0.76–0.93) for VF and EL, respectively. Additionally, both VF and EL have acceptable performances nearer the FFR cut point

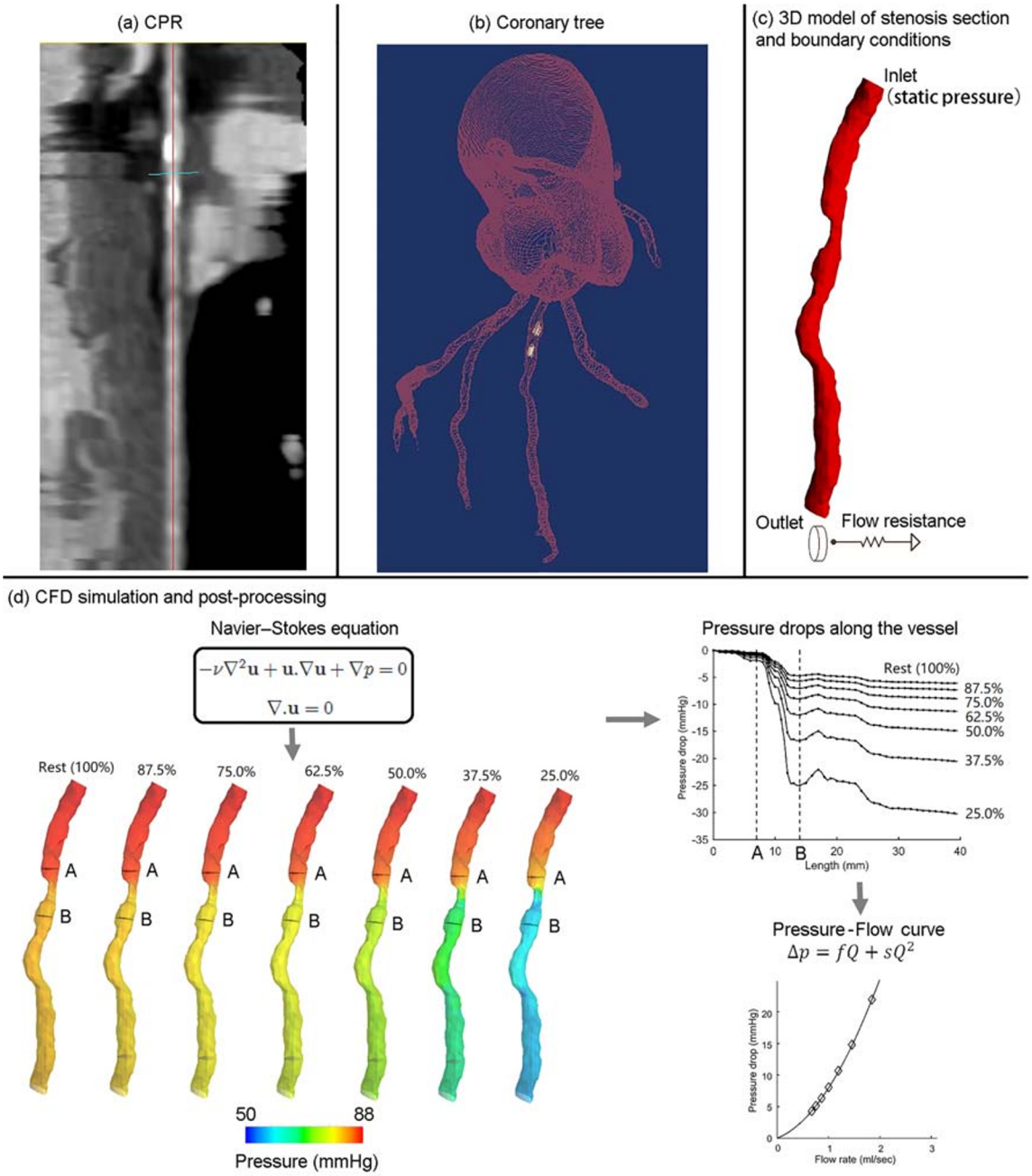

Fig. 1 Flow chart of the pressure-flow curve–based method. **a** CPR view of stenosis section. **b** 3D coronary tree model indicates the stenosis section and calcified plaques. **c** Only the stenosis section is retained for further CFD analysis. Static pressure (88 mmHg) is applied to the inlet and a lumped parameter model with only one resistance is coupled to the outlet. The "form–function" relationship is assumed to derive the values of resistance for each outlet with a given total resistance. Steady flow simulations are performed seven times, each with a different boundary condition (total distal resistance is set to be 120 mmHg s/cm^3 (to model rest condition) at first, and then reduced to 87.5, 75.0, 62.5, 50.0, 37.5, and 25.0%, respectively). **d** The pressure fields with different total distal resistances can be simulated with CFD method; then, pressure drops across the stenosis and flow rates with different total distal resistances are obtained; finally, the pressure drops and flow rates of these seven simulations were combined to provide a pressure-flow curve, and viscous friction (VF) and expansion loss (EL) are extracted from the curve

($0.75 < \text{FFR} \leq 0.85$). Correlation analysis demonstrated that the FFR values correlated well with VF (rho = − 0.74(95% CI − 0.83 to − 0.61, $p < 0.0001$) and EL (rho = − 0.74 (95% CI − 0.83 to − 0.61, $p < 0.0001$), as shown in Figs. 3 and 4.

Discussion

Pressure-flow curve derived from cCTA is a novel non-invasive method to assess hemodynamic significance of

Table 1 Patient demographics

Characteristic	Datum
Number of patients	58
Number of lesions	68
Ages (years)[a]	66.1 ± 10.4
Male	39 (67.2%)
Body mass index (kg/m^2)	24.37 ± 2.00
Cardiac risk factors	
Hypertension	20 (34.5%)
Hyperlipidemia	6 (10.3%)
Diabetes	9 (15.5%)
Smoking	18 (31.0%)
Symptoms	
Angina pectoris	37 (63.8%)
Probable angina pectoris	17 (29.3%)
Atypical chest pain	4 (6.9%)
Distribution of lesion[b]	
Left artery descending	47 (69.1%)
Right coronary artery	11 (16.2%)
Left circumflex artery	10 (14.7%)
Stenosis extent[b]	
< 50%	9 (13.2%)
50–69%	34 (50.0%)
≥ 70%	25 (36.8%)
Single-vessel disease	48 (82.8%)
Multi-vessel disease	10 (17.2%)

Unless otherwise specified, data are numbers of patients with percentages in parentheses

[a] Data are mean ± the standard deviation

[b] Data are numbers of lesions, with percentages in parentheses

coronary stenosis, which does not need to accurately estimate the distal flow resistance at maximal hyperemia. We have demonstrated the feasibility of assessing the hemodynamic significance of coronary artery stenoses through this cCTA-based method. Statistically significant correlations were also observed between the pressure-flow curve–derived parameters and invasive FFR. The major finding of the current study was that this new method enhanced diagnostic value of cCTA.

Over the past two decades, cCTA has developed into a valuable non-invasive diagnostic tool [17]. High diagnostic accuracy for detection of obstructive coronary stenosis was reported, and the negative predictive value reached up to 97% compared with ICA [6–8, 18]. However, the anatomical assessment correlated poorly with the hemodynamic severity of a coronary stenosis. Our study had similar findings for conventional cCTA parameters; no significant correlation was observed between invasive FFR and AS (rho = − 0.21, $p = 0.08$), and weak correlation was observed between invasive FFR and MLA (rho = 0.43, $p < 0.05$). Compared with functional testing (exercise electrocardiography, nuclear stress testing, or stress echocardiography), cCTA-based strategy did not improve clinical outcomes in symptomatic patients with suspected CAD [9]. Additionally, it was reported that even among severe stenoses confirmed by ICA, fewer than half were ischemia-causing stenoses [18]. These findings highlighted the need of a new technique to relate the complex relationship between the anatomical severity and hemodynamic severity.

FFR-CT has been validated against invasive FFR for detection of lesion-specific ischemia [19–21]. Especially with recent advances in machine learning–based pressure distribution calculation [22, 23] and flow-splitting method [24, 25], FFR-CT has developed into a more sophisticated approach for non-invasive evaluation of hemodynamic significance. However, little attention has been paid on the method used for estimating the hyperemia flow resistance. Generally speaking, allometric scaling law is used to estimate total coronary flow (under resting condition) from myocardial volume, and then, with the computed mean aortic pressure, resting flow resistance is calculated; finally, hyperemia flow resistance is modeled by simply reducing to 0.24 of the resting flow resistance [10]. Though empirical equations can be used to estimate the hyperemia flow resistances as described, it has substantial intrinsic limitations. Firstly, the myocardial volume changes a lot (up to 20%) during the cardiac cycle [11], making it difficult to accurately estimate the resting flow resistances; secondly, there are large interindividual variations in the magnitude of adenosine-induced changes in microvascular resistances [12], making it difficult to accurately model the hyperemia flow resistance. Recent meta-analysis studies

Table 2 Results of assessment for VF, EL, AS, and MLA (per vessel analysis). *VF*, viscous friction; *EL*, expansion loss; *AS*, area stenosis; *MLA*, minimal lumen area

	FFR ≤ 0.8 ($n = 31$)	FFR > 0.8 ($n = 37$)	p value
VF (mmHg s/ml)[a]	1.89 (0.54–2.66)	0.32 (0.14–0.34)	$p < 0.0001$
EL (mmHg s^2/ml^2) [a]	3.08 (0.48–4.71)	0.37 (0.12–0.30)	$p < 0.0001$
AS (%)[b]	64.29 ± 14.16	56.91 ± 13.70	$p = 0.0328$
MLA (mm^2)[a]	3.32 (2.67–4.20)	5.56 (3.42–6.67)	$p = 0.0009$

[a] Date are medians, with the first to third quartile in parentheses

[b] Data are means ± standard deviations

Table 3 Results for pressure-flow curve–based method in detecting significant stenosis (defined as FF ≤ 0.80). *VF*, viscous friction; *EL*, expansion loss

	Overall ($n = 68$)		0.75 < FFR ≤ 0.85 ($n = 25$)	
	VF (95% CI)	EL (95% CI)	VF (95% CI)	EL (95% CI)
Sensitivity	0.87 (0.70–0.96)	0.81 (0.62–0.92)	0.79 (0.49–0.94)	0.71 (0.42–0.90)
Specificity	0.89 (0.75–0.97)	0.92 (0.77–0.98)	0.91 (0.57–0.99)	0.91 (0.57–0.99)
Positive predictive value (PPV)	0.87 (0.69–0.96)	0.89 (0.71–0.97)	0.91 (0.60–0.99)	0.91 (0.57–0.99)
Negative predictive value (NPV)	0.89 (0.74–0.96)	0.85 (0.69–0.94)	0.77 (0.46–0.94)	0.71 (0.42–0.90)

reported that notable decrease of the diagnostic accuracy of FFR-CT was observed for lesions within the gray zone [26, 27]. Despite there is a reproducibility "problem" for invasive FFR in the gray zone [28], the uncertainty in estimating hyperemia flow resistance would also play an important role. Since CFD-based results are used as the ground truth, the same problem also exists in the machine learning–based approach. Brian et al reported an alternative approach to estimate the boundary conditions based on the structural deformation of coronary lumen and aorta [29]. However, uncertainty still exists in the estimation of outlet flow resistances. Additionally, four cardiac phases (at 70%, 80%, 90%, and 99% of R-R interval) of cCTA images were used, which would limit its in-hospital utilization.

Recently, our group combined CDP with CFD and proposed a new non-invasive approach for assessing hemodynamic significance of coronary stenosis, which would fully character the pressure-flow behavior of a stenosis [14]. Other than FFR, CDP was an alternate invasive diagnostic parameter for determining the functional significance of a stenosis [30, 31]. Since it was based on both pressure and flow information, submaximal hyperemia or in the presence of microvascular dysfunction would have less impact on it [32–34]. However, due to ignoring the viscous friction effect, the measured values in basal and hyperemic conditions still had differences [32]. Also, reliable measurement of flow velocity was technically difficult. Fortunately, these limitations of CDP could be overcome by combining with CFD method. With the simulated pressure-flow curve, both the viscous friction and expansion loss can be estimated (making it independent of estimated flow resistance), and by employing the CFD method, the flow rate can be simulated accurately. From the results, both VF and EL show high sensitivity and specificity. Though the sensitivity of VF and EL decreases nearer the FFR cut point (0.75 < FFR ≤ 0.85), the specificity remains high. Through ROC curve analyses, we find that the ability of indicating ischemic coronary lesions is significantly improved by VF and EL, compared with cCTA alone.

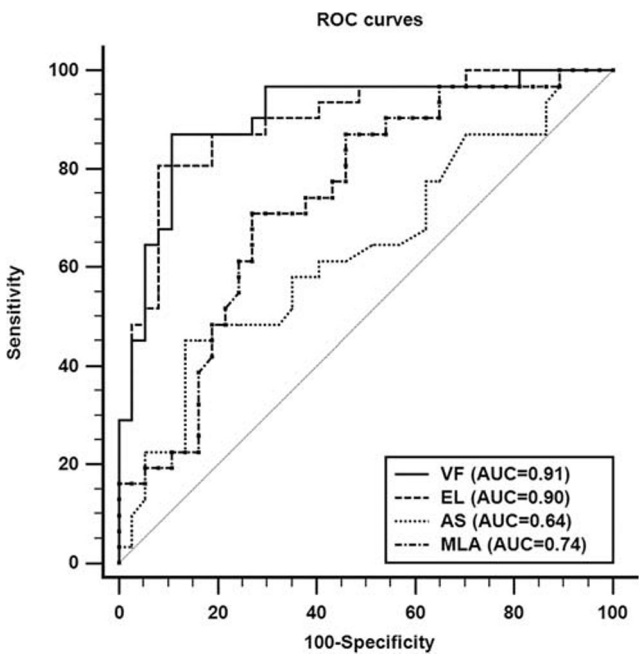

Fig. 2 Receiver operating characteristic curves for the detection of lesion-specific ischemia by viscous friction (VF), expansion loss (EL), area stenosis (AS), and minimal lumen area (MLA) using FFR at a threshold of 0.80 as the reference standard

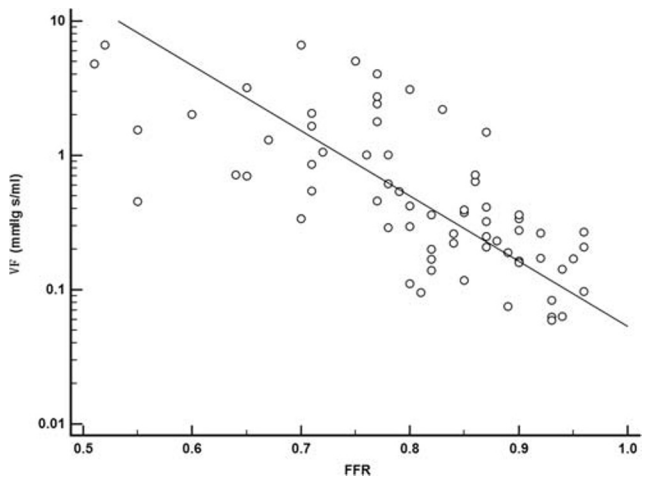

Fig. 3 Correlation of the viscous friction (VF) with invasive FFR

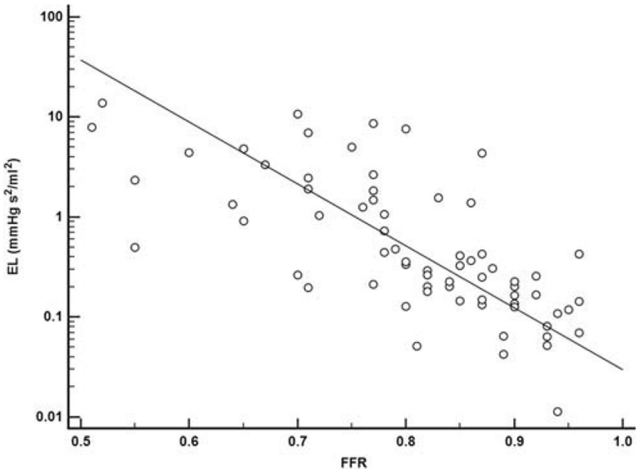

Fig. 4 Correlation of the expansion loss (EL) with invasive FFR

In theoretical, given hyperemia flow rate Q, the pressure drop can be calculated with VF and EL (by using Eq. (1)), and then FFR can also be obtained. However, in coronary circulation, flow rate is dependent not only on the epicardial coronary arteries but also on the distal microcirculation, which could not be directly quantified from cCTA images. More recently, a completely different approach based on the pressure-flow curve was proposed by Panagiotis et al [35, 36]. Since the hyperemia flow rate could not be estimated accurately, they used a range of hyperemia flow rates to further obtain a normalized pressure-flow curve, and the ratio of the area under this curve to a reference area was defined (virtual functional assessment index, vFAI) to distinguish hemodynamically significant lesions from non-significant lesions [36]. Despite the CFD models they used did not include any side branches, the diagnostic accuracy still reached 0.93 [36]. By combining a range of "inaccuracy" hyperemia flow rate, the method proposed by Panagiotis et al calculates the "average" FFR. This is diametrically opposed to our method. Without knowing the accurate hyperemia flow rate, we employ the pressure curve–based parameters charactering the property of local (regional) flow resistance to assess lesion-specific ischemia. Although a slightly lower diagnostic accuracy was reported in this study, we believe these two different purely anatomy-derived methods can be combined together to improve the current performance. Further head-to-head comparison studies between these two methods are also needed.

Study limitations

There are several limitations in this study. First, only patients who underwent both a cCTA and invasive angiography (within 2 weeks) were evaluated, leading to inclusion bias. Second, heavily calcified lesions presented a challenge for the 3D anatomic modeling, and were excluded in this study. Maybe by using more advanced lumen segmentation method would further improve the ability to deal with heavily calcified lesions. Also, further investigation about the influence of calcium score on diagnostic performance of the proposed method is needed. Third, the number of analyzed vessels was small, and the cutoff values for VF and EL need to be further validated. Fourth, the pressure-flow curve–based method was not compared with FFR-CT, and the diagnostic performance for intermediate stenosis was still unknown. Head-to-head comparison with FFR-CT needs to be further performed. Fifth, we did not exclude diabetics and further investigation about the performance of the proposed method for patients with and without diabetes is also needed. Finally, due to the retrospective nature of this study, no outcome data is reported which is based on the revascularization decisions made by the pressure-flow curve–based method. Further prospective studies are also required to confirm current findings.

Conclusions

In conclusion, a purely anatomy-derived non-invasive method for detection of hemodynamically significant stenosis, pressure-flow curve derived from cCTA, was evaluated in 68 lesions. Results demonstrated that it was superior to cCTA alone for detecting ischemia-causing stenosis.

Funding information This study has received funding by the National Natural Science Foundation of China (Grant No. 61601368), the Fundamental Research Funds for the Central Universities (No. 3102018ZY021) and the Discipline promotion project of Xijing hospital (No. XJZT18MJ52).

Compliance with ethical standards

Guarantor The scientific guarantor of this publication is Minwen Zheng.

Conflict of interest The authors of this manuscript declare no relationships with any companies whose products or services may be related to the subject matter of the article.

Statistics and biometry No complex statistical methods were necessary for this paper.

Informed consent Written informed consent was obtained from all subjects (patients) in this study.

Ethical approval Institutional Review Board approval was obtained.

Methodology
- Retrospective
- Diagnostic or prognostic study
- Performed at one institution

References

1. Pijls NHJ, Sels J-WEM (2012) Functional measurement of coronary stenosis. J Am Coll Cardiol 59:1045–1057
2. Fearon WF, Nishi T, De Bruyne B et al (2018) Clinical outcomes and cost-effectiveness of fractional flow reserve-guided percutaneous coronary intervention in patients with stable coronary artery disease: three-year follow-up of the FAME 2 trial (Fractional Flow Reserve Versus Angiography for Multive). Circulation 137: 480–487
3. Tonino PAL, De Bruyne B, Pijls NHJ et al (2009) Fractional flow reserve versus angiography for guiding percutaneous coronary intervention. N Engl J Med 360:213–224
4. De Bruyne B, Fearon WF, Pijls NHJ et al (2014) Fractional flow reserve–guided PCI for stable coronary artery disease. N Engl J Med 371:1208–1217
5. Pothineni NV, Shah NS, Rochlani Y et al (2016) U.S. trends in inpatient utilization of fractional flow reserve and percutaneous coronary intervention. J Am Coll Cardiol 67:732–733
6. Miller JM, Rochitte CE, Dewey M et al (2008) Diagnostic performance of coronary angiography by 64-row CT. N Engl J Med 359: 2324–2336
7. Meijboom WB, Meijs MFL, Schuijf JD et al (2008) Diagnostic accuracy of 64-slice computed tomography coronary angiography. A prospective, multicenter, multivendor study. J Am Coll Cardiol 52:2135–2144
8. Budoff MJ, Dowe D, Jollis JG et al (2008) Diagnostic performance of 64-multidetector row coronary computed tomographic angiography for evaluation of coronary artery stenosis in individuals without known coronary artery disease. Results from the prospective multicenter ACCURACY. J Am Coll Cardiol 52:1724–1732
9. Douglas PS, Hoffmann U, Patel MR et al (2015) Outcomes of anatomical versus functional testing for coronary artery disease. N Engl J Med 372:1291–1300
10. Taylor CA, Fonte TA, Min JK (2013) Computational fluid dynamics applied to cardiac computed tomography for noninvasive quantification of fractional flow reserve: scientific basis. J Am Coll Cardiol 61:2233–2241
11. Ashikaga H, Coppola BA, Yamazaki KG et al (2008) Changes in regional myocardial volume during the cardiac cycle: implications for transmural blood flow and cardiac structure. Am J Physiol Heart Circ Physiol 295:610–618
12. Mejía-Rentería H, Lauri FM, Lee JM et al (2019) Interindividual variations in the adenosine-induced hemodynamics during fractional flow reserve evaluation: implications for the use of quantitative flow ratio in assessing intermediate coronary stenoses. J Am Heart Assoc 8:e012906
13. Young DF, Tsai FY (1973) Flow characteristics in models of arterial stenoses — I. Steady flow. J Biomech 6:395–402
14. Xie X, Zheng M, Wen D, Li Y, Xie S (2018) A new CFD based non-invasive method for functional diagnosis of coronary stenosis. Biomed Eng Online 17:36
15. De Bruyne B, Pijls NH, Barbata E et al (2003) Intracoronary and intravenous adenosine 5′-triphosphate, adenosine, papaverine, and contrast medium to assess fractional flow reserve in humans. Circulation 107:1877–1883
16. DeLong ER, DeLong DM, Clarke-Pearson DL (1988) Comparing the areas under two or more correlated receiver operating characteristic curves: a nonparametric approach. Biometrics 44:837–845
17. Van Mieghem CAG (2017) CT as gatekeeper of invasive coronary angiography in patients with suspected CAD. Cardiovasc Diagn Ther 7:189–195
18. Meijboom WB, Van Mieghem CAG, van Pelt N et al (2008) Comprehensive assessment of coronary artery Stenoses. Computed tomography coronary angiography versus conventional coronary angiography and correlation with fractional flow reserve in patients with stable angina. J Am Coll Cardiol 52:636–643
19. Koo BK, Erglis A, Doh JH et al (2011) Diagnosis of ischemia-causing coronary stenoses by noninvasive fractional flow reserve computed from coronary computed tomographic angiograms. Results from the prospective multicenter DISCOVER-FLOW (Diagnosis of Ischemia-Causing Stenoses Obtained Via Noni). J Am Coll Cardiol 58:1989–1997
20. Nakazato R, Park HB, Berman DS et al (2013) Noninvasive fractional flow reserve derived from computed tomography angiography for coronary lesions of intermediate stenosis severity: results from the DeFACTO study. Circ Cardiovasc Imaging 6:881–889
21. Norgaard BL, Leipsic J, Gaur S et al (2014) Diagnostic performance of noninvasive fractional flow reserve derived from coronary computed tomography angiography in suspected coronary artery disease: the NXT trial (Analysis of Coronary Blood Flow Using CT Angiography: Next Steps). J Am Coll Cardiol 63: 1145–1155
22. Yu M, Lu Z, Shen C et al (2019) The best predictor of ischemic coronary stenosis: subtended myocardial volume, machine learning–based FFR CT, or high-risk plaque features? Eur Radiol 29:3647–3657
23. Coenen A, Kim Y-H, Kruk M et al (2018) Diagnostic accuracy of a machine-learning approach to coronary computed tomographic angiography–based fractional flow reserve. Circ Cardiovasc Imaging 11:e007217
24. Han H, Bae YG, Hwang ST et al (2019) Computationally simulated fractional flow reserve from coronary computed tomography angiography based on fractional myocardial mass. Int J Cardiovasc Imaging 35:185–193
25. Tang CX, Liu CY, Lu MJ et al (2019) CT FFR for ischemia-specific CAD with a new computational fluid dynamics algorithm. JACC Cardiovasc Imaging. https://doi.org/10.1016/j.jcmg.2019.06.018
26. Celeng C, Leiner T, Maurovich-Horvat P et al (2019) Anatomical and functional computed tomography for diagnosing hemodynamically significant coronary artery disease. JACC Cardiovasc Imaging 12:1316–1325
27. Cook CM, Petraco R, Shun-Shin MJ et al (2017) Diagnostic accuracy of computed tomography-derived fractional flow reserve a systematic review. JAMA Cardiol 2:803–810
28. Petraco R, Sen S, Nijjer S et al (2013) Fractional flow reserve-guided revascularization: practical implications of a diagnostic gray zone and measurement variability on clinical decisions. JACC Cardiovasc Interv 6:222–225
29. Ko BS, Cameron JD, Munnur RK et al (2017) Noninvasive CT-derived FFR based on structural and fluid analysis: a comparison with invasive FFR for detection of functionally significant stenosis. JACC Cardiovasc Imaging 10:663–673
30. Banerjee RK, Ashtekar KD, Effat MA et al (2009) Concurrent assessment of epicardial coronary artery stenosis and microvascular dysfunction using diagnostic endpoints derived from fundamental fluid dynamics principles. J Invasive Cardiol 21:511–517
31. Banerjee RK, Ashtekar KD, Helmy TA, Effat MA, Back LH, Khoury SF (2008) Hemodynamic diagnostics of epicardial coronary stenoses: in-vitro experimental and computational study. Biomed Eng Online 7:24
32. Kolli KK, Effat MA, Peelukhana SV et al (2014) Hyperemia-free delineation of epicardial and microvascular impairments using a basal index. Ann Biomed Eng 42:1681–1690

33. Kolli KK, van de Hoef TP, Effat MA et al (2016) Diagnostic cutoff for pressure drop coefficient in relation to fractional flow reserve and coronary flow reserve: a patient-level analysis. Catheter Cardiovasc Interv 87:273–282
34. Hebbar UU, Effat MA, Peelukhana SV, Arif I, Banerjee RK (2017) Delineation of epicardial stenosis in patients with microvascular disease using pressure drop coefficient: a pilot outcome study. World J Cardiol 9:813–821
35. Anagnostopoulos CD, Siogkas PK, Liga R et al (2019) Characterization of functionally significant coronary artery disease by a coronary computed tomography angiography-based index: a comparison with positron emission tomography. Eur Heart J Cardiovasc Imaging 0:1–9
36. Siogkas PK, Anagnostopoulos CD, Liga R et al (2019) Noninvasive CT-based hemodynamic assessment of coronary lesions derived from fast computational analysis: a comparison against fractional flow reserve. Eur Radiol 29:2117–2126